*Journal of Applied Pharmaceutical Research*
*Volume 13 Issue 1, Year of Publication 2025, Page 38 – 48*
*DOI: https://doi.org/10.69857/joapr.v13i1.783*

Check for updates

**Research Article**

***JOURNAL OF APPLIED PHARMACEUTICAL RESEARCH*** | ***JOAPR***
***www.japtronline.com*** ***ISSN: 2348 – 0335***

# *EXPLORING THE STRUCTURAL ASPECTS OF ALANINE RACEMASE ENZYME FOR ANTITUBERCULAR DRUG DISCOVERY – A COMPUTATIONAL APPROACH*

Unni Jayaram*, Parthan Anilkumar, Fathima Rifana Yousuf, Graceson Jose

***Article Information***
Received: 17th November 2024
Revised: 21st January 2025
Accepted: 16th February 2025
Published: 28th February 2025

**Keywords**
*Alanine racemase, tuberculosis, Mycobacterium tuberculosis, protein crystal structure, antitubercular agents*

***ABSTRACT***
**Background:** Tuberculosis (TB) is a communicable disease that is a significant cause of ill health and one of the leading causes of death worldwide. The current antibiotics have been pivotal in managing TB to a greater extent. Still, the issue of antitubercular drug resistance is indeed a matter of concern and requires effective drug discovery strategies targeting less explored targets. One of the less explored but promising antitubercular targets, Alanine racemase (AlaR), a prokaryotic enzyme providing the essential peptidoglycan precursor *D*-alanine (*D*-Ala) in bacterial cell wall synthesis, is an attractive target for antitubercular drug discovery. **Objective:** The current study aims to explore the available protein targets of the AlaR enzyme in Mycobacterium tuberculosis and to understand the structural aspects to be followed in designing inhibitors for them. **Methodology:** As a part of the study, the crystal structure of the alanine racemase enzyme from Mycobacterium tuberculosis was subjected to computational studies using the Schrodinger drug design suite. The significant protocols followed involved protein preparation and fragment-based drug design studies. **Results and discussion:** The in-silico data suggested that substituted pteridine derivatives, which impart stable interaction at the active site of the alanine racemase enzyme, may be the potential lead moiety for drug design. **Conclusion:** Although the preliminary screening suggests that the pteridine ring system may be a promising lead, detailed *in silico* studies must be carried out, such as molecular mechanic generalized born surface area (MM-GBSA), density functional theory (DFT) studies, induced fit docking, molecular dynamics, etc. for further authentication. For effective correlation, detailed in vivo studies on AlaR enzyme inhibition can be carried out from a future perspective.

## *INTRODUCTION*

The bacterial disease tuberculosis (TB) usually spreads from one person to another through airborne transmission. The causative agent for this global threat is the *tubercle bacillus, Mycobacterium tuberculosis*. The disease is rarely transmitted from infected cows to humans by drinking non-sterilized milk. The disease may affect any organ; however, pulmonary TB is the most prevalent and infectious [1].

*Department of Pharmaceutical Chemistry, Caritas College of Pharmacy, Ettumanoor – 686 631, Kerala, India

***For Correspondence:** **jayaramkvt2@gmail.com**

As per the latest World Health Organization (WHO) report of 2022, 21.4 lakh cases of TB were notified in India in 2021. The increase was 18 % more than that reported in 2020. The report explained the impact of coronavirus disease 2019 (COVID-19) in enhancing the burden of TB disease in a worldwide scenario. WHO further quotes that TB is considered to be the 13$^{th}$ leading cause of death and the 2$^{nd}$ leading cause of infection after COVID-19. An estimated number of 1.6 million people lost their life to TB in 2021. It was further estimated that around 10.6 million people fell ill with TB worldwide, including 06 million men, 3.4 million women, and 1.2 million children. Even though the disease is preventable and curable, it occurs in all age groups and all countries. Adding to the burden, multidrug-resistant TB (MDR-TB) is now found to be a public health crisis and global threat. The report shows only 1 out of 3 patients with MDR-TB assessed treatment in 2021 [2].

The currently marketed drugs such as D-cycloserine, isoniazid, rifampin, pyrazinamide, ethambutol, and streptomycin have limited therapeutic action against TB due to resistance developed towards known strains. D-cycloserine is commercially used among the known alanine racemase (AlaR) inhibitors as antitubercular agents. Still, their utility is limited due to severe toxic side effects arising from the lack of specificity of the target. The experimental evidence suggests that this toxicity is mainly attributed to the partial agonistic action of the drug towards N-methyl-D-aspartate (NMDA) receptors and glycine site. Yet another concern is the inhibitory action of *D*-cycloserine towards some other pyridoxal-5'-phosphate (PLP) dependent enzymes such as aspartate racemase, serine racemase, and arginine racemase, which are involved in the metabolism and biosynthesis of $\gamma$-aminobutyric acid (GABA) neurotransmitter. Since *D*-cycloserine is not a specific inhibitor of AlaR but can inhibit several PLP-dependent enzymes, more than one mechanism leading to *D*-cycloserine resistance is likely to occur. Other known AlaR inhibitors face the same issue of lack of target specificity. Hence, drug-resistant TB is now a global threat and requires a more significant health focus and research measures [3].

The bacterial AlaR is a potent and largely unexploited antibacterial drug target for antibacterial drug discovery. It is a PLP-dependent enzyme that plays a key role in cell wall synthesis in prokaryotes [4]. Biochemically, the enzyme causes the conversion of *L*-alanine to *D*-alanine, which is utilized by bacteria for peptidoglycan synthesis. The target is expressed in both gram-positive and gram-negative bacteria. Being absent in higher eukaryotes, AlaR can be considered a promising target to assure selectivity and specificity in action. The homodimeric enzyme consists of a PLP cofactor with alanine, lysine, and tyrosine amino acids in the catalytic binding pocket. The narrow entryway to the binding domain is a significant challenge in designing novel molecules as potent inhibitors [5]. However, small molecule inhibitors with maximal interaction with binding site amino acid residues may ensure target selectivity and specificity with potent inhibitory action [5].

Over the past decade, computer-aided drug design has played a prominent role in exploring target enzyme crystal structures, thereby facilitating the design and discovery of potent inhibitors [6]. The structure-based drug design approach in this genre was able to dive into the crystal structures of known proteins/ enzymes and figure out the structural requirements of ligands/ inhibitors for developing novel drug candidates. The approach also supported effective scaffold designing in a customized target to ensure specificity and selectivity towards the concerned enzyme [7]. Through this study, an attempt has been made to understand the known and reported crystal structures of the AlaR enzyme available from *mycobacterium tuberculosis.* Our primary focus was on the high-resolution crystal structure of AlaR *Mycobacterium tuberculosis* with PDB ID: 1XFC, which can be explored for structure-based drug discovery for designing and developing novel antitubercular drugs. The challenges and pitfalls in drug design for the enzyme will also be discussed for effective drug discovery measures.

## *MATERIALS AND METHODS*

### *In Silico* studies

The *in silico* studies were performed using the Schrodinger drug design suite installed on an Intel Xeon E3 3.7 GHz processor, 16 GB RAM HP Z238 micro tower workstation functioning on a Linux platform.

### Protein preparation

The protein data bank retrieved the x-ray crystallography-derived structures of the target AlaR enzyme from Mycobacterium tuberculosis (PDB ID: 1XFC, resolution 1.9 Å). The protein was prepared using the Protein Preparation Wizard tool in Schrodinger suite 2023-3 [7]. The structures were pre-processed to assign the bond orders and zero-order bonds to

metals. The missing side chains were added, and the break-up in protein structures was repaired using the Prime module [8]. Energy minimization of protein structures was performed using the OPLS-2005 force field [9]. The crystallographic water molecules with less than three hydrogen bonds were deleted because such molecules were considered irrelevant, further smoothening the computational approach. However, water molecules 426, 489, 543, and 551 in 1XFC were retained, showing hydrogen bonding interaction with the cofactor. The H-bonds were assigned, keeping the crystal symmetry, and minimization was performed until the convergence of heavy atoms reached 0.30 Å RMSD.

**Fragment-based drug design**

A fragment library consisting of 1500 fragments was docked in XP mode into the catalytic pocket of *Mycobacterium tuberculosis* AlaR (PDB ID: 1XFC). Based on their binding affinity in the catalytic pocket, molecular weight, and druglike properties, 70 fragments were selected [7]. These selected fragments were grown into molecules with different linkers. The developed molecules were optimized with the Ligprep module, and low-energy conformers were docked in extra precision mode into the catalytic pocket of *Mycobacterium tuberculosis* AlaR (PDB ID: 1XFC) [10]. A flowchart summarizing the computational approach is hereby provided in Figure 1 for better understanding.

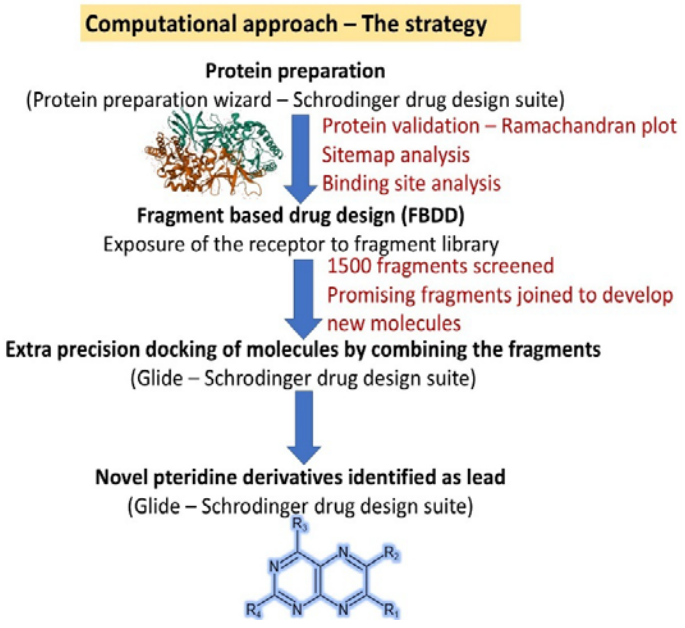


**Figure 1: The adopted computational strategy for antitubercular drug discovery involving the fragment-based drug design approach**

***RESULTS AND DISCUSSIONS***

**Crystal structures of alanine racemase from *Mycobacterium tuberculosis***

In 2005, LeMagueres P et al. reported the crystal structure of M. tuberculosis AlaR (PDB ID: 1XFC) isolated by x-ray diffraction method with a resolution of 1.90 Å [5]. The crystal structure was reported to be a dimer with 384 residues in each monomer (Figure 2). The catalytic domain was similar to that of AlaR from *Bacillus stearothermophilus* and *Pseudomonas aeruginosa* [4, 11]. The crystal structure comprised of $\alpha/\beta$ barrel at the *N*-terminus (1-246 residues) and $\beta$ strands (247-384 residues) at the *C*-terminus.

The PLP cofactor is covalently bonded to Lys42 residue at the binding site by internal aldimine bond. The relatively low root mean square deviation (RMSD) of *C* alpha ($C_\alpha$) atoms (0.56 Å) ensured the crystallographic symmetry of constituent monomers. To guide the structure-based drug design approach, the active site cavity had a dimension of approximately 5.5 Å × 5.0 Å × 2.5 Å, lying adjacent to the PLP cofactor. The active site is constituted by amino acid residues such as methionine (Met319), lysine (Lys42), tyrosine (Tyr46), and Tyr364. The binding pocket is also constituted by tryptophan (Trp88), which reduces the free space in the cavity along with two water molecules. The oxygen (O3') of PLP interacts with one of the water molecules (Wat203), forming a bond with NE1 of Trp88. The opposite monomer amino acid residues glutamine (Gln321') and asparagine (Asp320') also interact with these 2 water molecules. Due to the compact binding site, a designed inhibitor with a molecular weight of up to 300 daltons can accommodate the active pocket, but it is difficult to reach due to the constricted entryway made by two residues, Tyr271' and Tyr364.

The authors suggested that these two residues must move apart to ensure the entry of small molecule inhibitors for effective inhibitory action. The authors further claimed that although designing a potent inhibitor of *M. tuberculosis* AlaR is challenging, it will ensure novelty and action against tuberculosis. The crystal structure can be further utilized for structure-based drug designing of novel molecules as the binding site is confirmed to be the clinical target of the standard drug *D*-Cycloserine. The *M. tuberculosis* AlaR has structural similarity with that of *Geobacillus stearothermophilus* alanine racemase (*G. stearothermophilus* AlaR) and *Pseudomonas aeruginosa* alanine racemase (*P. aeruginosa* AlaR).

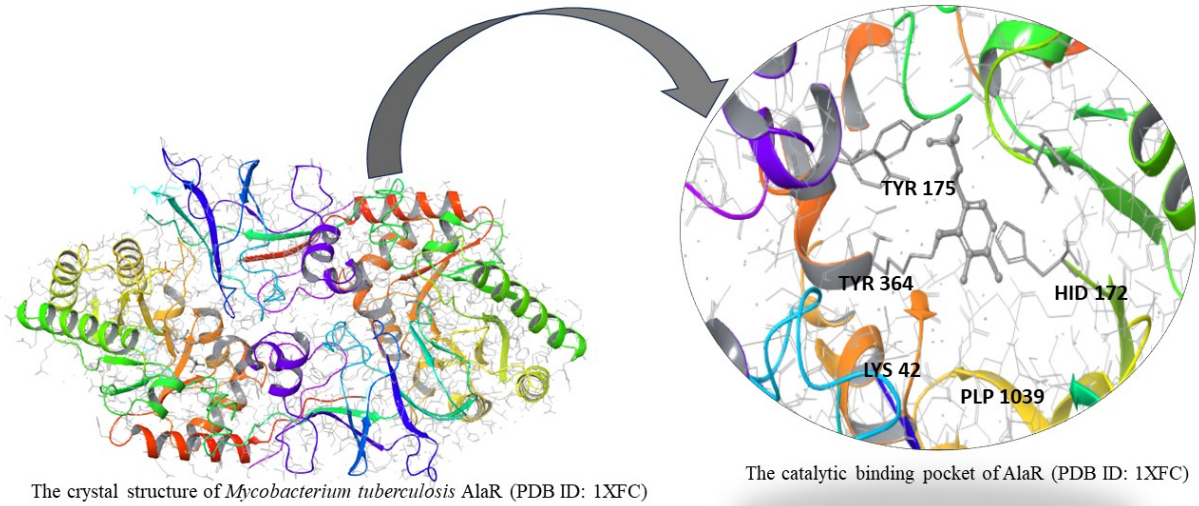


**Figure 2: The crystal structure of *Mycobacterium tuberculosis* AlaR with catalytic binding pocket consisting of PLP cofactor.** The key amino acid residues responsible for mechanistic action are highlighted

**Protein preparation and validation**

The 3D X-ray crystal structures of the AlaR enzyme from *M. tuberculosis* (PDB ID: 1XFC, 1.9 Å) were retrieved from the protein data bank (PDB). The SiteMap program in the Schrödinger molecular modeling suite was used to generate the five most active sites of selected proteins. The site score, D score, and pocket volume of the generated sites of AlaR (PDB ID: 1XFC) were calculated and shown in Table 1. The siteMap details of the most favorable pocket have been shown in Table 2. The SiteMap generated active site was the same as that of the selected catalytic pocket for the docking protocol, as shown in Figure 3.

The SiteMap_1XFC_site_2, with a site score of 0.897028 and a Dscore of 1.027344, was considered to be the most favorable site. The Dscore usually ranges from 0 - 1, where the higher score suggests a better binding domain region. Similarly, the pocket volume in the range of 100 – 1000 Å3 is considered to be a favorable parameter. The selected SiteMap also satisfies it (258.622 $Å^3$) with proper interactions exhibited at the target site. The site score is yet another crucial parameter in SiteMap analysis in order to evaluate the binding site within the receptor. It provides an overall score for ranking sites based on physical and chemical properties. The site score range of 0.8 – 1.0 suggests druggable site which may require further optimization. The most favourable site (SiteMap_1XFC_site_2) however exhibited the site score value of 0.897028 which is the highest when compared to other sites generated. The SiteMap analysis of the targets confirmed that the catalytic pocket is constituted by the cofactor PLP and other key amino acid residues like Lys42, Tyr46, Tyr364, arginine (Arg228), isoleucine (Ile231) and glycine (Gly230) as in case of AlaR *M. tuberculosis*. The binding site is constituted by both hydrophilic (including hydrogen bond acceptors (red) and the hydrogen bond donors (blue)) and hydrophobic residues. This suggests that the balance of hydrophobic and polar groups in ligand structure is required for the enzyme inhibitory activity.

The PDB IDs for AlaR (4A3Q, 1XFC and 1SFT) from *S*taphylococcus *aureus* (*S. aureus*), *M. tuberculosis* and *B. stearothermophilus* respectively were overlayed (Figure 4) to analyze the catalytic binding pockets of the enzyme [12]. The RMSD of superimposition between AlaR *S. aureus* (PDB ID: 4A3Q) and AlaR *M. tuberculosis* (PDB ID: 1XFC) was found to be 1.803 Å with an alignment score of 0.131. The RMSD of superimposition between AlaR *S. aureus* (PDB ID: 4A3Q) and AlaR *B. stearothermophilus* (PDB ID: 1SFT) was found to be 1.228 Å with an alignment score of 0.061. The AlaR catalytic

pocket structural similarity among different strain of bacteria is thus evident. The RMSD calculation is often considered to be crucial in quantifying the crystal structure similarity especially in terms of binding site. The AlaR enzyme is widely spread across prokaryotes including gram positive and negative bacteria which makes it an attractive target for drug discovery studies. As evidenced, low RMSD indicates high structural similarity, while a higher RMSD is indicative of some serious deviations in structures. Similarly, RMSD value below 2 Å suggests good similarity for the catalytic binding domain. The designed inhibitors thus would be able to impart maximal activity towards other microorganisms concerned with AlaR enzyme.

**Table 1: The SiteMap details of AlaR (PDB ID: 1XFC)**

| SiteMap | Site score | Size (Å) | Dscore | Volume (Å$^3$) |
|---|---|---|---|---|
| sitemap_1XFC_site_2 | 0.897028 | 455 | 1.027344 | 258.622 |
| sitemap_1XFC_site_1 | 0.894504 | 588 | 1.006422 | 375.242 |
| sitemap_1XFC_site_5 | 0.892848 | 275 | 1.027224 | 178.703 |
| sitemap_1XFC_site_4 | 0.887061 | 300 | 1.015085 | 170.128 |
| sitemap_1XFC_site_3 | 0.868652 | 335 | 0.983821 | 182.819 |

**Table 2**. The SiteMap details of the most favourable site of AlaR (PDB ID: 1XFC).

| SiteMap | Site Score | Size (Å) | Dscore | Volume (Å$^3$) | [1]Hb Accept area (Å$^2$) | [2]Hb Donor area (Å$^2$) | [3]Hphilic surface area (Å$^2$) | [4]Hphobic surface area (Å$^2$) |
|---|---|---|---|---|---|---|---|---|
| sitemap_1XFC_site_2 | 0.897028 | 455 | 1.027344 | 258.622 | 1379.216 | 2819.167 | 4159.224 | 197.639 |

Notes: [1]hydrogen bond acceptor area; [2]hydrogen bond donor area; [3]hydrophilic surface area; [4]hydrophobic surface area.

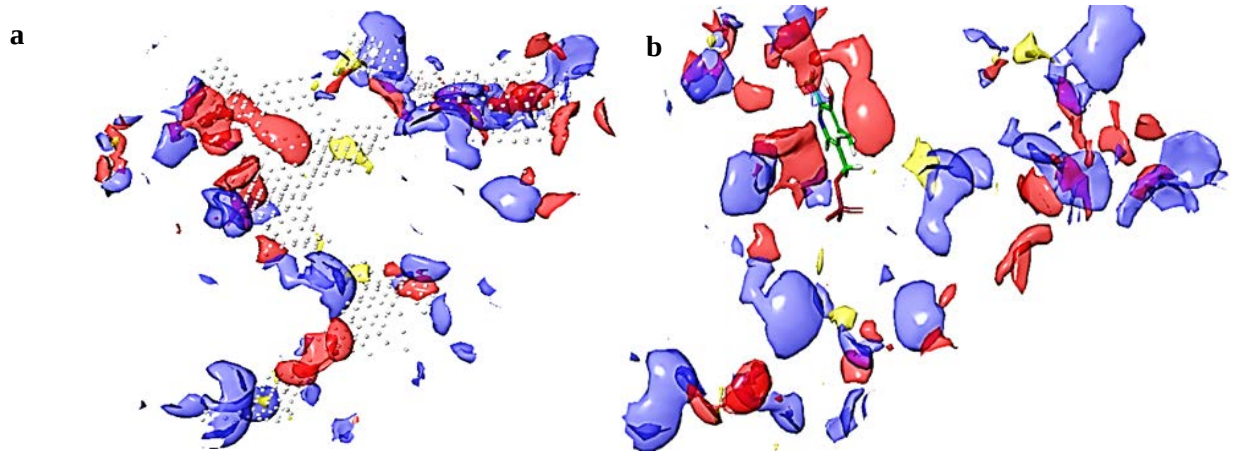


**Figure 3**. a) The most favorable SiteMap generated for AlaR (PDB ID: 1XFC) enzyme. b) The siteMap overlay over the AlaR crystal structure (PDB ID: 1XFC) with PLP cofactor confirming the actual site of binding

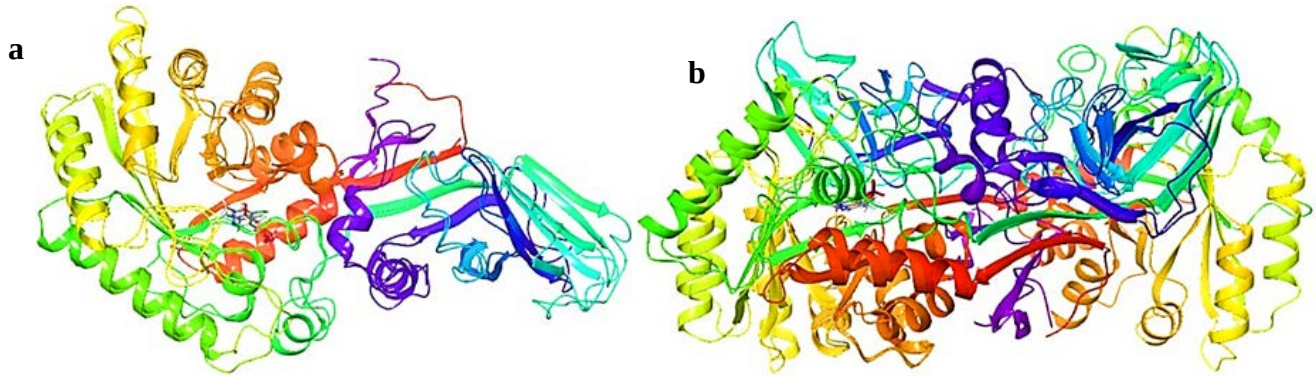


**Figure 4**. a) Superimposition of 4A3Q and 1XFC (RMSD: 1.803 Å, alignment score: 0.131). b) Superimposition of 4A3Q and 1SFT (RMSD: 1.228 Å, alignment score: 0.061).

The protein preparation wizard module in the Schrödinger suite was utilized to prepare the enzymes for further *in silico* studies. Energy minimization was performed using the OPLS-2005 force field, which is integrated into the Schrödinger suite, making it more user-friendly. Compared to other force fields like CHARMM or AMBER, it ensures more accuracy in small molecule parameterization with improved solvation-free energy predictions. The missing loops and residues were added using the prime module in the Schrödinger suite. Water molecules 426, 489, 543, and 551 in 1XFC were retained, showing hydrogen bonding interaction with respective cofactors. The Ramachandran plots further validated all the prepared protein crystal structures. In the case of 1XFC, 95.8% of the total 382 amino acid residues were found to be in the acceptable regions (Figure 5). No residues, except glycine and proline, were found in the unacceptable areas. This ensures the quality of receptor structure for docking analysis as most of the amino acid residues are in favorable areas with minimal steric hindrance and energetically favorable angles. At the same time, very few (Glycine and proline) are found to be in disallowed regions, usually due to steric clashes.

**Fragment based drug design**

A fragment-based drug design approach was performed utilizing the fragment library by Schrödinger and Maestro in Phase [13]. The fragment library of 1500 fragments was grown into molecules using 70 selected fragments and linkers. Based on extra precision glide score, glide emodel, glide energy and binding free energy (MM-GBSA) values, the molecules were further designed and evaluated. The Phase database of fragment structures was utilized for FBDD studies. It allows multiple fragment databases to be screened using single-screen calculation. The program ensures the screening of small molecules, typically less than 300 Da, and clogs P<3, which typically bind to the target with high binding affinity. The FBDD, in turn, is advantageous in identifying fragment-sized molecules than lead-sized or drug-sized molecules, by which the chemical space can be explored much more efficiently. The promising fragments can be combined and modified by adding additional functional groups and substituents to yield potent lead molecules. The docking score of selected combined fragments through the FBDD approach is shown in Table 3. The binding poses at the active site of 1XFC of selected molecules developed by the FBDD approach are shown in Figure 6. The top ranked lead molecules with their docking score and interacting amino acid residues are summarized in Table 4.

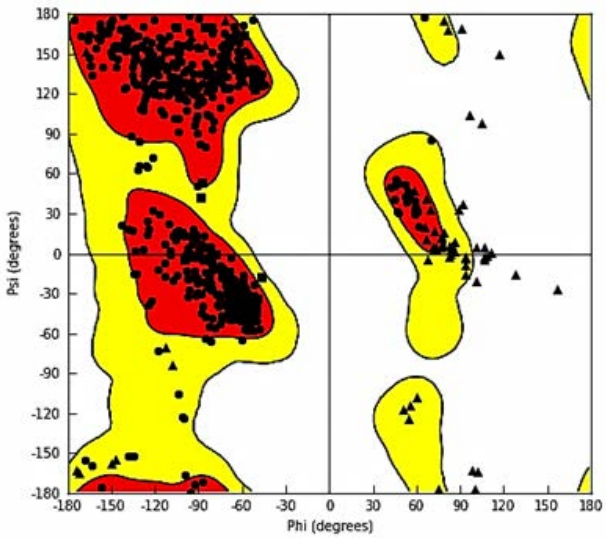


**Figure 5: The Ramachandran plot of AlaR (PDB ID: 1XFC) confirming the correctness of the prepared receptor structure for docking analysis**

**Table 3**. The docking score of the designed molecules against *M. tuberculosis* AlaR (PDB ID: 1XFC).

| S. No. | Combined fragments | Docking score |
|---|---|---|
| 1 | fragment_join-1 :: J93 (frag 17) :: JTADO3 (frag 2) | -5.12 |
| 2 | fragment_join-1 :: 3f (frag 2) :: fragment_join-1 :: J93 (frag 3) :: JDA84 (frag 5) | -4.82 |
| 3 | fragment_join-1 :: J93 (frag 28) :: 3f (frag 2) | -4.64 |
| 4 | fragment_join-1 :: 3f (frag 2) :: fragment_join-1 :: J93 (frag 28) :: 3f (frag 3) | -4.61 |
| 5 | fragment_join-1 :: J93 (frag 28) :: 3f (frag 3) | -4.46 |
| 6 | fragment_join-1 :: J93 (frag 28) :: JTADO10 (frag 2) | -4.31 |
| 7 | fragment_join-1 :: JDA88 (frag 6) :: JDA87 (frag 5) | -4.16 |
| 8 | fragment_join-1 :: J93 (frag 28) :: JTADO16 (frag 2) | -4.05 |
| 9 | fragment_join-1 :: JDA88 (frag 6) :: JDA87 (frag 6) | -3.98 |
| 10 | fragment_join-1 :: 3f (frag 2) :: fragment_join-1 :: J93 (frag 28) :: 3f (frag 3)-2 | -3.95 |

| S. No. | Combined fragments | Docking score |
|---|---|---|
| 11 | fragment_join-1 :: JTADO16 (frag 2) :: fragment_join-1 :: J93 (frag 28) :: 3f (frag 2) | -3.93 |
| 12 | fragment_join-1 :: J93 (frag 26) :: JDA87 (frag 1) | -3.92 |
| 13 | fragment_join-1 :: JDA87 (frag 11) :: JDA8 (frag 3) | -3.92 |
| 14 | fragment_join-1 :: 3f (frag 2) :: fragment_join-1 :: J93 (frag 19) :: JDA84 (frag 1) | -3.88 |
| 15 | fragment_join-1 :: 3f (frag 2) :: fragment_join-1 :: J93 (frag 18) :: JDA84 (frag 5) | -3.86 |
| 16 | fragment_join-1 :: J93 (frag 3) :: JDA84 (frag 5) | -3.81 |
| 17 | fragment_join-1 :: J93 (frag 3) :: JDA84 (frag 1) | -3.63 |
| 18 | fragment_join-1 :: J93 (frag 14) :: 3f (frag 2) | -3.54 |
| 19 | fragment_join-1 :: J93 (frag 19) :: JDA84 (frag 1) | -3.52 |
| 20 | fragment_join-1 :: J93 (frag 26) :: JDA84 (frag 5) | -3.49 |
| 21 | fragment_join-1 :: J93 (frag 13) :: 3f (frag 2) | -3.48 |
| 22 | fragment_join-1 :: 3f (frag 2) :: fragment_join-1 :: J93 (frag 25) :: JDA84 (frag 1) | -3.46 |
| 23 | fragment_join-1 :: J93 (frag 18) :: JDA84 (frag 5) | -3.45 |
| 24 | fragment_join-1 :: J93 (frag 25) :: JDA84 (frag 5) | -3.42 |
| 25 | fragment_join-1 :: J93 (frag 26) :: J93 (frag 6) | -3.39 |
| 26 | fragment_join-1 :: JTADO10 (frag 2) :: fragment_join-1 :: J93 (frag 28) :: 3f (frag 2) | -3.39 |
| 27 | fragment_join-1 :: J93 (frag 28) :: 3f (frag 3)-2 | -3.36 |
| 28 | fragment_join-1 :: J93 (frag 25) :: JDA84 (frag 1) | -3.35 |
| 29 | fragment_join-1 :: J93 (frag 3) :: JDA84 (frag 1)-2 | -3.33 |
| 30 | fragment_join-1 :: J93 (frag 26) :: 3f (frag 3) | -3.15 |
| 31 | fragment_join-1 :: JTADO20 (frag 1) :: JTADO3 (frag 2) | -3.14 |
| 32 | fragment_join-1 :: J93 (frag 25) :: 3f (frag 3) | -3.11 |
| 33 | fragment_join-1 :: 3f (frag 2) :: fragment_join-1 :: J93 (frag 18) :: 3f (frag 3) | -3.03 |
| 34 | fragment_join-1 :: JTADO3 (frag 3) :: JTADO3 (frag 2) | -2.89 |
| 35 | fragment_join-1 :: JTADO12 (frag 1) :: J93 (frag 2) | -2.75 |
| 36 | fragment_join-1 :: J93 (frag 25) :: JTADO3 (frag 2) | -2.73 |
| 37 | fragment_join-1 :: J93 (frag 18) :: JTADO3 (frag 2) | -2.73 |
| 38 | fragment_join-1 :: JTADO3 (frag 3) :: JTADO3 (frag 2)-2 | -2.7 |
| 39 | fragment_join-1 :: J93 (frag 18) :: 3f (frag 3) | -2.7 |
| 40 | fragment_join-1 :: J93 (frag 6) :: JDA87 (frag 5) | -2.63 |
| 41 | fragment_join-1 :: JDA84 (frag 3) :: J93 (frag 2) | -2.63 |
| 42 | fragment_join-1 :: JTADO3 (frag 1) :: 3f (frag 2) | -2.55 |
| 43 | fragment_join-1 :: J93 (frag 19) :: 3f (frag 2) | -2.45 |
| 44 | fragment_join-1 :: JTADO3 (frag 3) :: J93 (frag 6) | -2.42 |
| 45 | fragment_join-1 :: JDA84 (frag 3) :: JTADO3 (frag 2) | -2.39 |
| 46 | fragment_join-1 :: 3f (frag 2) :: fragment_join-1 :: J93 (frag 18) :: JTADO3 (frag 2) | -2.33 |
| 47 | fragment_join-1 :: JDA84 (frag 4) :: J93 (frag 2) | -2.08 |
| 48 | fragment_join-1 :: JDA84 (frag 4) :: JTADO3 (frag 2) | -1.97 |
| 49 | fragment_join-1 :: J93 (frag 18) :: 3f (frag 2) | -1.93 |
| 50 | fragment_join-1 :: J93 (frag 6) :: JDA87 (frag 6) | -1.21 |

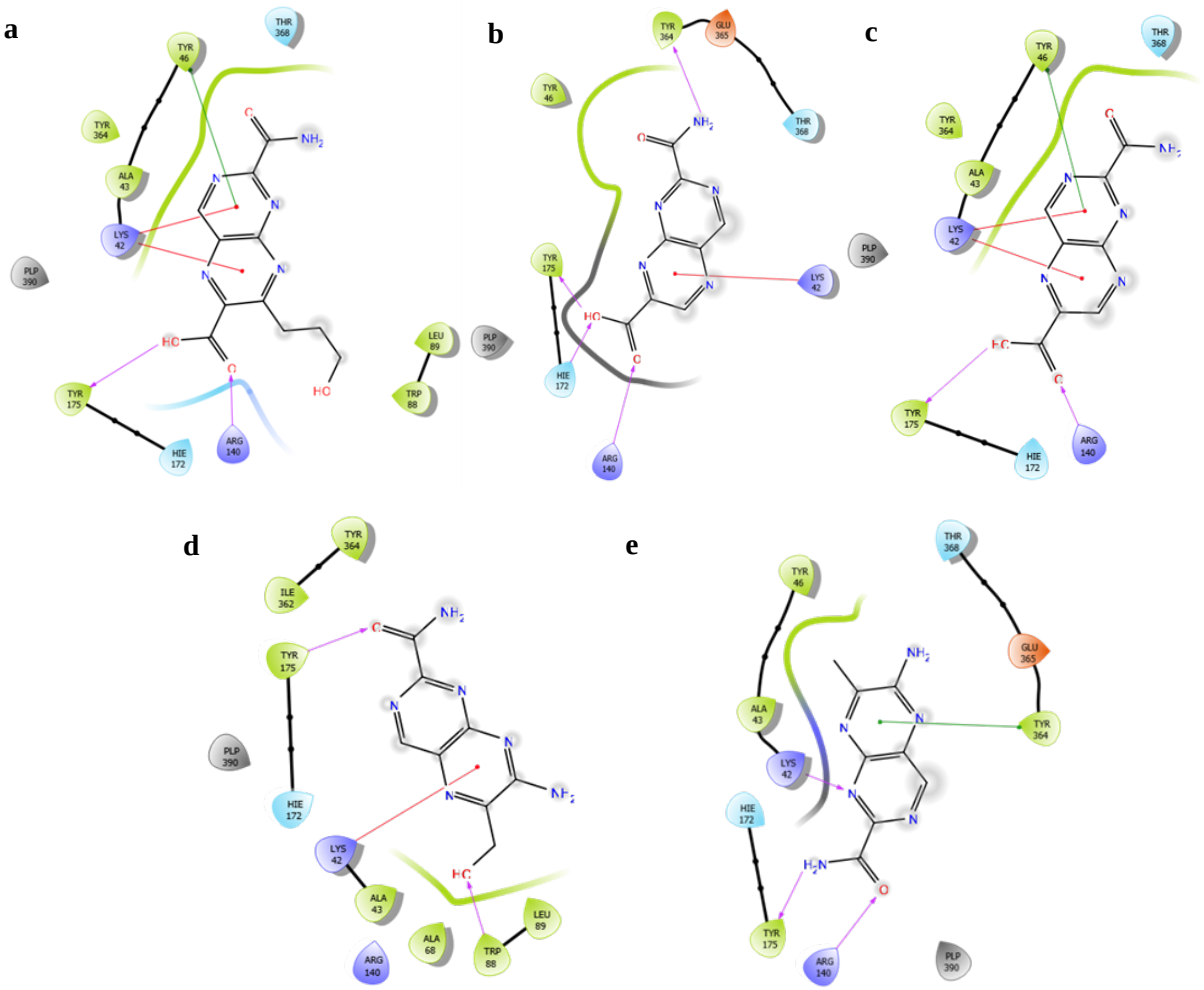


**Figure 6: The binding poses and interaction of some selected molecules developed by fragment-based drug design approach within the catalytic pocket of AlaR (PDB ID: 1XFC).** The hydrogen bonding (Purple line), π – cationic interaction (Red line), and π – π stacking interaction (Green line) among the molecule and binding site amino acid is depicted in the figure.

**Table 4: The top ranked molecules with their docking score and interacting amino acid residues developed by the fragment-based drug design approach.**

| Top ranked molecules | Docking score | Interacting amino acid residues | Types of interaction observed |
|---|---|---|---|
| Molecule 1 | -5.12 | Tyr46; Lys42; Tyr175; Arg140 | Hydrogen bonding; π-π stacking; π-cationic |
| Molecule 2 | -4.82 | Lys42; Arg140; Hie172; Tyr175 | Hydrogen bonding; π-cationic |
| Molecule 3 | -4.64 | Lys42; Tyr46; Arg140; Tyr175 | Hydrogen bonding; π-π stacking; π-cationic |
| Molecule 4 | -4.61 | Lys42; Trp88; Tyr175 | Hydrogen bonding; π-cationic |
| Molecule 5 | -4.46 | Lys42; Arg140; Tyr175; Tyr364 | Hydrogen bonding; π-π stacking |

The lead molecules exhibited extra precision (XP) docking score in the range of -4.46 to -5.12. The molecular mechanics – generalized born surface area (MM – GBSA) scores were -35.92 to -75.65 kcal $mol^{-1}$. These scores exceeded the standard inhibitors docked towards the same target site. To validate the docking protocol, in the absence of any co-crystal ligand, the PLP cofactor present at the binding site was rocked, which exhibited the same interactions with amino acid residues (Lys42, Arg228, Trp88, Tyr364, Tyr46, Ile231, Ser213, and Gly230) as that of the experimental data suggested. Additionally, the SiteMap analysis perfectly predicted the binding site involving the same cofactor and the amino acid residues of interest.

**Scaffold and drug designing approach**

The detailed fragment-based drug design studies led to an interpretative finding that the pteridine ring system (Figure 7) with substituents at 2nd ($R_4$), 4th ($R_3$), 6th ($R_2$) and 7th ($R_1$) position will be a potent scaffold for antibacterial activity. The potency is attributed by the fact that a 2-ring system (basic pteridine nucleus) fits well into the catalytic binding pocket of AlaR *M. tuberculosis*. Moreover, the stable $\pi$-cationic interaction is exhibited by the aromatic ring with some key catalytic pocket amino acid residues like Lys42, Tyr 46 and Tyr364 which plays crucial role in inhibitory action. The positioning of -$CONH_2$ substituent with electron withdrawing nature at 2nd position ($R_4$) is found to be important in imparting stable hydrogen bonding interaction with residues like Arg140, Tyr175 and Tyr364. The functional moiety -COOH and -$CH_2OH$ at the opposite end to carbamide group on the other adjacent ring in pteridine at 7th position ($R_2$) enhances the bulkiness of molecules and imparts a stable hydrogen bonding interaction with catalytic pocket residues like tryptophan (Trp88), Tyr175, Arg140 and histidine (His172). The $\pi$-$\pi$ stacking interaction of the pteridine ring (either 1st or 2nd ring system) with aromatic amino acid residues like Tyr364 and Tyr46 further adds to ensured stability and flexibility of designed ligand molecules at the catalytic pocket. Docking studies also suggested that 6th position ($R_1$) substitution with varied groups doesn't much contribute to stable interactions. Since, the results of fragment-based drug designing approach didn't highlighted the need for any substitution at 4th position ($R_3$), fixing any substituent at the concerned position was ignored. The perfect hydrophobic-hydrophilic balance offered by the molecule due to pteridine ring (hydrophobic – orange colour) and $R_1$-$R_4$ substituents (hydrophilic – cyan colour) ensures stable interactions within in the catalytic pocket that may finally ensure inhibitory activity towards the target enzyme.

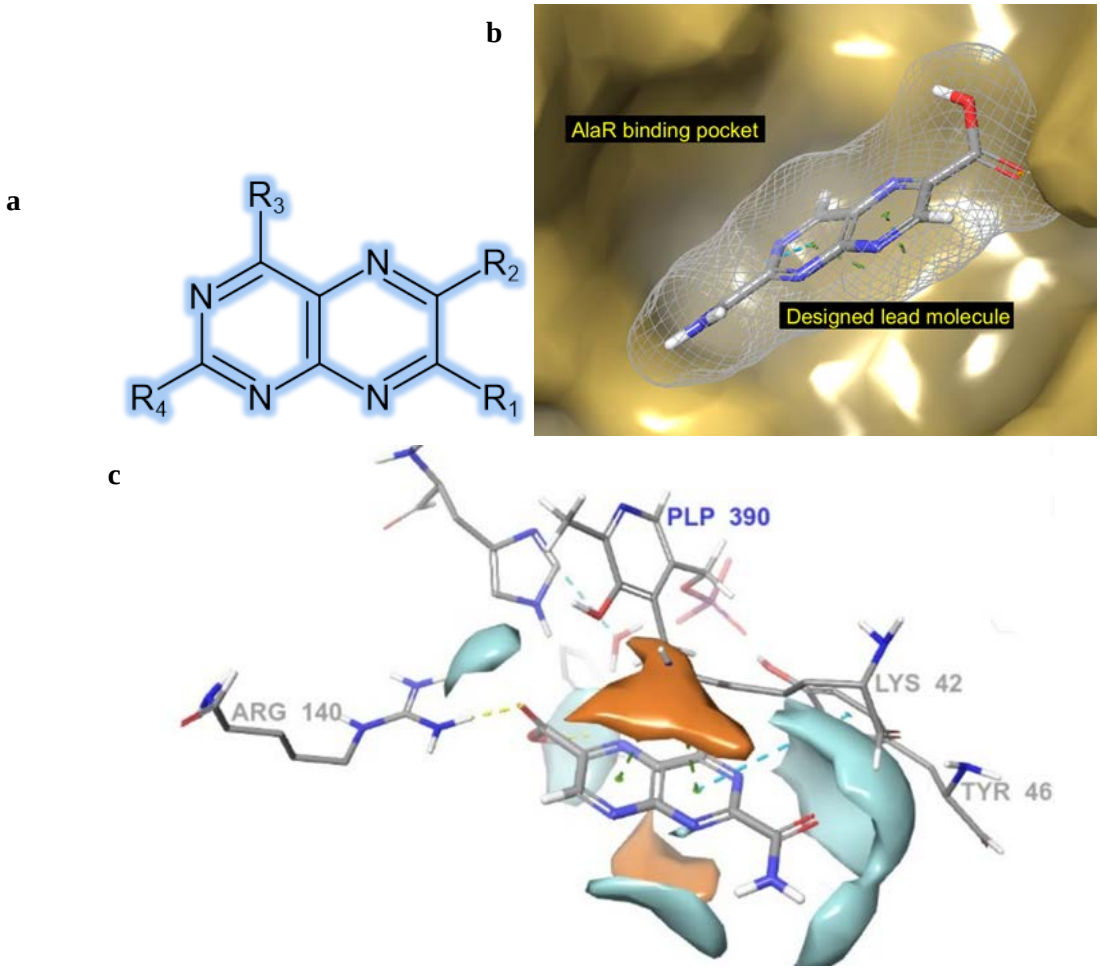


**Figure 7**. a) The structural representation of pteridine ring system developed by fragment-based drug design approach assuring potent inhibitory activity towards AlaR *M. tuberculosis* (1XFC). b) The designed lead molecule fitting correctly at the AlaR *M. tuberculosis* catalytic binding pocket. c) The hydrophobic (orange) – hydrophilic (cyan) mapping of designed molecules with interaction at the catalytic binding pocket of AlaR.

**Need for further *in silico* evaluation**

Although the *in silico* methods adopted here have been well optimized for the drug discovery scenario, the dynamicity of the receptor is questionable, which would then play a crucial role in interaction efficiency. The advanced approaches of induced fit docking and molecular dynamics of pteridine derivatives towards the AlaR should be carried out further for validation. However, the aspects of fragment-based drug design, which is considered to be relatively new and underexplored, shed light on the interaction patterns of designed leads and also were able to establish the key interaction features such as hydrogen bonding and hydrophobicity among the concerned ligand-receptor complex. The adopted *in silico* protocols could also correlate the activity of designed leads and the role of interacting amino acid residues, typically Lys42 and Tyr46, in the racemization mechanism of this PLP-dependent enzyme.

**Pteridine derivatives as potent lead molecules**

The 2-ring system pteridine lead molecules are considered a perfect fit into the catalytic binding domain of AlaR with some significant molecular interactions with active site amino acid residues. In comparison to the known inhibitors such as *D*-cycloserine and *O*-carbamoyl-*D*-serine, the planarity exhibited in the pteridine derivative adds to its ability to undergo hydrophobic interactions such as π-π stacking interactions with aromatic residues like Tyr175 and Trp88 in the active site. The four nitrogen atoms involved in the ring system add to the ability of an overall molecule to undergo prominent hydrogen bonding interactions with amino acid residues like Lys42 and Arg140. One of the key structural features of pteridine derivatives to undergo keto-enol tautomerism helps the lead to establish proper spatial alignment, making it a good fit in the catalytic binding site. The discussed structural aspects are considered significant compared to the limited known inhibitors where the required structural complexity is not observed, exhibiting limited specificity and selectivity.

## *CONCLUSION*

Antibiotic resistance is a burning issue that leads to an increment in the total mortality rate and ill health among healthy individuals. An effective approach to overcome this scenario is identifying, targeting, and developing potent antibacterial agents with effective action toward inhibiting potential bacterial targets, which might be less explored but promising. When it comes to tuberculosis, multidrug resistance and frequent exposure to usual drugs cause ineffectiveness and reduced therapeutic action. The alanine racemase enzyme ubiquitously expressed in prokaryotes is a promising anti-mycobacterial target for drug design. Here, the fragment-based drug design approach was utilized to identify some substituted pteridine derivatives as *Mycobacterium tuberculosis* AlaR inhibitors with significant antimycobacterial action. On further structural and chemical analysis, the contribution of the 2-ring system and substitution of the ring, predominantly at the C2 and C7 positions, were explored, which led to the fact that the concerned scaffold is a perfect fit in the catalytic binding pocket. Moreover, stable hydrogen bonding, π-cationic, and π-π stacking interactions with the key amino acid residues (Lys42, Tyr46, and Tyr364) in the catalytic binding pocket may ensure site-specific and selective inhibitory action. Although the study suggests some significant overlook on inhibitory potential towards *Mycobacterium tuberculosis* AlaR, advanced *in silico* approaches like molecular mechanic generalized born surface area (MM-GBSA), density functional theory (DFT) studies, induced fit docking, molecular dynamics, etc., have to be carried out for assured evaluation of antitubercular activity in future. In addition, the *in vitro* assessment by AlaR enzyme inhibitory assay and Alamar blue assay must be carried out for compelling activity correlation. The *in silico*-*in vitro*-*in vivo* correlation at the end will give us a clear picture regarding the utility of designed inhibitors as potential leads and drug discovery thereafter.

## *ACKNOWLEDGEMENTS*

The author would like to thank Caritas intramural research project scheme 2023 (CHIHS/RDC/CP-01/2023, dated 26/7/2023), research and development cell, Caritas Hospital and Institute of Health Sciences, Thellakom, Kottayam, for the financial support provided.

## *FINANCIAL ASSISTANCE*

NIL

## *CONFLICT OF INTEREST*

The authors declare no conflict of interest.

## *AUTHOR CONTRIBUTION*

Unni Jayaram performed the literature survey, collected the data, performed the experimental part, and wrote the research paper. Parthan Anilkumar and Fathima Rifana Yousuf made the maximum effort in corrections and conducted a literature survey for the introductory part of a research paper. Graceson Jose

performed data mining related to in silico studies and framed the experimental section of a research paper. All authors checked the final draft.

## *REFERENCES*


[1] Alsayed SSR, Gunosewoyo H. Tuberculosis: Pathogenesis, Current Treatment Regimens and New Drug Targets. *Int J Mol Sci*., **8**, 5202 (2023). https://doi.org/10.3390/ijms24065202.

[2] Mustansir AA, Gupta V, Addanki RND, Mannava AS, Parashar KD. A cross-sectional study to assess stigma associated with tuberculosis in patients, family members, and health care staff in central India. *Indian J Tuberc*., **71**, S237-S244 (2024). https://doi.org/10.1016/j.ijtb.2024.04.001.

[3] Aguilar Diaz JM, Abulfathi AA, Te Brake LH, Van Ingen J, Kuipers S, Magis-Escurra C, Raaijmakers J, Svensson EM, Boeree MJ. New and repurposed drugs for the treatment of active tuberculosis: an update for clinicians. *Respiration*., **102**, 83-100 (2023). https://doi.org/10.1159/000528274.

[4] Shimizu-Ibuka A, Sato A, Ichimura H, Hiraga H, Nakayama S, Nishiwaki, T. Regulation of alanine racemase activity by carboxylates and the d-type substrate d-alanine. *FEBS J*., **290**, 2954-2967 (2023). https://doi.org/10.1111/febs.16745.

[5] De Chiara C, Prosser GA, Ogrodowicz R, de Carvalho LPS. Structure of the *D*-cycloserine-resistant variant D322N of alanine racemase from *Mycobacterium tuberculosis*. *ACS Bio Med Chem Au*., **3**, 233-239 (2023). https://doi.org/10.1021/acsbiomedchemau.2c00074.

[6] Roney M, Mohd Aluwi MF. The importance of *in-silico* studies in drug discovery. *Intell Pharm*., **2**, 578-579 (2024). https://doi.org/10.1016/j.ipha.2024.01.010.

[7] Chang Y, Hawkins BA, Du JJ, Groundwater PW, Hibbs DE, Lai F. A guide to *in silico* drug design. *Pharmaceutics*., **15**, 49 (2022). https://doi.org/10.3390/pharmaceutics15010049.

[8] Alturki NA, Mashraqi MM, Alzamami A, Alghamdi YS, Alharthi AA, Asiri SA, Ahmad S, Alshamrani S. *In-Silico* Screening and Molecular Dynamics Simulation of Drug Bank Experimental Compounds against SARS-CoV-2. *Molecules*., **27**, 4391 (2022). https://doi.org/10.3390/molecules27144391.

[9] Yue K, Doherty B, Acevedo O. Comparison between Ab Initio Molecular Dynamics and OPLS-Based Force Fields for Ionic Liquid Solvent Organization. *J Phys Chem B*., **126**, 3908-3919 (2022). https://doi.org/10.1021/acs.jpcb.2c01636.

[10] Lokwani DK, Sarkate AP, Karnik KS, Nikalje APG, Seijas JA. Structure-Based Site of Metabolism (SOM) Prediction of Ligand for CYP3A4 Enzyme: Comparison of Glide XP and Induced Fit Docking (IFD). *Molecules*., **25**, 1622 (2022). https://doi.org/10.3390/molecules25071622.

[11] Lemar G, Far F. A. D. Homology Modeling of Bifunctional Enzyme Alanine Racemase from *Taibaiella Chishuiensis*. *Biosci Biotech Res Asia*., **17** (2020). https://doi.org/10.13005/bbra/2864.

[12] Dong H, Hu T, He G, Lu D, Qi J, Dou Y, Long W, He X, Ju J, Su D. Structural features and kinetic characterization of alanine racemase from Bacillus pseudofirmus OF4. *Biochem Biophys Res Commun*., **497**, 139-145 (2018). https://doi.org/10.1016/j.bbrc.2018.02.041.

[13] Li Q. Application of fragment-based drug discovery to versatile targets. *Front Mol Biosci*., **7** (2020). https://doi.org/10.3389/fmolb.2020.00180